Available online at www.sciencedirect.com
SCIENCE DIRECT®
Journal of Sound and Vibration 279 (2005) 1203–1217
JOURNAL OF SOUND AND VIBRATION
www.elsevier.com/locate/jsvi

Short Communication

Vibrations of cracked rotor system: transverse crack versus slant crack

A.S. Sekhar*, A.R. Mohanty, S. Prabhakar

Department of Mechanical Engineering, Indian Institute of Technology, Kharagpur 721 302, India

Received 16 July 2003; accepted 26 January 2004

Available online 23 September 2004

1. Introduction

Propagating fatigue cracks can have detrimental effects on the reliability of the rotating machinery such as turbomachinery, process machinery, etc. Dynamic analysis of cracked rotors has been a subject of great interest for the last three decades and excellent reviews on this are available in Refs. [1–4].

All the works reported in Refs. [1–4] consider mainly the transverse crack that occurs from the fatigue of the shaft material due to an excessive bending moment. However, Ichimonji and Watanabe [5] considered a slant crack that occurs from the fatigue of the shaft due to the torsional moment, and studied the dynamics of a simple rotor for qualitative analysis. Ichimonji et al. [6] extended their work and presented using 3D finite element method (FEM), a qualitative analysis for the rotor with slant crack. Sekhar and Balaji [7] have developed the stiffness matrix of an element having slant crack and using FEM, analyzed the rotor system for steady-state response. Further studies on slant cracked rotor system are available on condition monitoring in Ref. [8] and on transient analysis in Ref. [9].

The detection and monitoring of slant crack in the rotor system using mechanical impedance has been presented in this paper. The paper also synthesizes several works of the authors on cracked rotors to compare the two types of shaft cracks while studying flexural vibration

*Corresponding author. Tel.: +91-3222-55221; fax: +91-3222-55303.
E-mail address: sekhar@mech.iitkgp.ernet.in (A.S. Sekhar).

0022-460X/$ - see front matter
doi:10.1016/j.jsv.2004.01.011

Nomenclature

$[C]$	flexibility matrix with crack
$[D]$	matrix includes gyroscopic effects and damping
D	diameter of shaft
e	unbalance eccentricity of the rotor
F	amplitude of impulse force
$[K]$	stiffness matrix
l	element length
L	length of the rotor
$[M]$	mass matrix
q	vector of nodal quantities
Q	force vector
X	location of the crack from left bearing
X_f	location of force from left bearing
Z_c	mechanical impedance of the cracked rotor-bearing system
Z_0	mechanical impedance of the rotor-bearing system without the crack
Z_c/Z_0	normalized mechanical impedance
α	depth of the crack
$\bar{\alpha}$	relative crack depth, α/D
ω, Ω	operating speed
ω_{op}	instant operating speed
ω_T	torsional frequency

characteristics. Eigenvalue analysis; steady state and transient response; crack detection based on changes in mechanical impedance and wavelet techniques have been discussed in order to compare slant crack with transverse crack.

2. Modelling of cracks

2.1. Transverse crack

There are several ways to model the transverse crack as mentioned in Refs. [2–4]. In the present study, the flexibility matrices of the cracked section as given in [10] are utilized for crack modelling (see Fig. 1). During the shaft's rotation, the crack opens and closes (the breathing action of the crack) depending on the rotor deflection [11]. For a large class of machines, the static deflection is much greater than the rotor vibration. With this assumption the crack is closed when $\phi = 0$ and it is fully open when $\phi = \pi$ (see Fig. 2). The transverse surface crack on the shaft element introduces considerable local flexibility due to strain energy concentration in the vicinity of the crack tip under the load. The additional strain energy due to the crack results in a local flexibility matrix C_c, which will be C_{op} and C_{HC} for a fully open crack and half-open, half-closed condition respectively.

The dimensionless compliance coefficients in C_c, are functions of non-dimensional crack depth, $\bar{\alpha}(\alpha/D)$, where α is the crack depth in shaft diameter D (see Fig. 1). These compliance coefficients are computed from the derivations discussed in Refs. [10,11]. The total flexibility matrix for the cracked section is given as [11]

$$[C] = [C_0] + [C_c], \tag{1}$$

where $[C_0]$ consists of the flexibility coefficients for an element without crack. As explained before, C_c will be C_{op} or C_{HC} depends on the breathing position of crack (see Fig. 2).

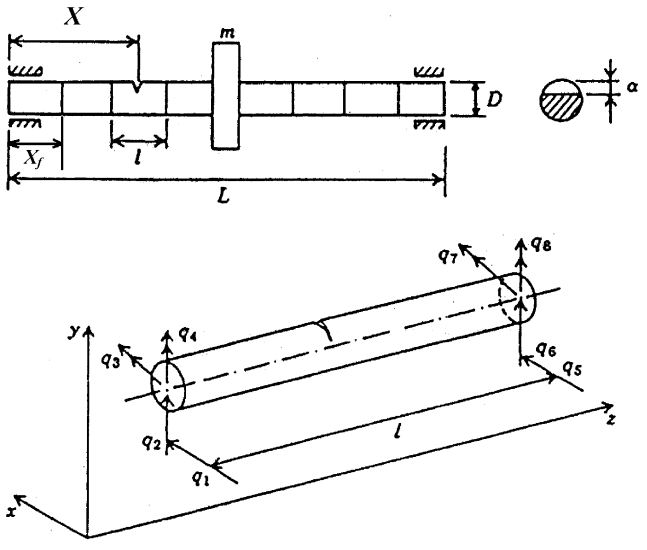

Fig. 1. Rotor system with a transverse cracked element.

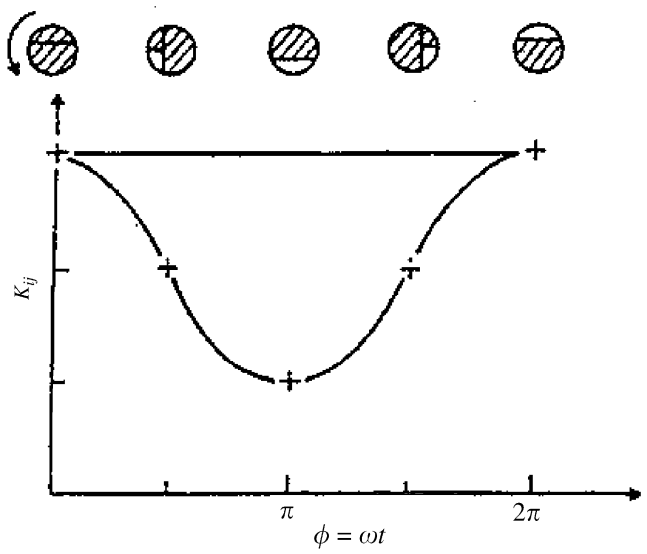

Fig. 2. Breathing crack model for transverse crack.

2.1.1. Stiffness matrix

The stiffness matrix of the cracked element is written as [11]

$$[K_c] = [T][C]^{-1}[T]^{\mathrm{T}}, \tag{2}$$

where $[T]$ is the transformation matrix. When the shaft is cracked, during the rotation the stiffness varies with time, or with angle. The variation may be expressed by a truncated cosine series

$$[K] = [K_0] + [K_1]\cos\ \omega t + [K_2]\cos\ 2\omega t + [K_3]\cos\ 3\omega t + [K_4]\cos\ 4\omega t, \tag{3}$$

where $[K_\eta]$, $\eta = 0, 1, \ldots, 4$, are fitting coefficient matrices, determined from the known behavior of the stiffness matrix at certain angular locations [11]. These are obtained from the compliance matrices C_o, C_{op} and C_{HC} together with Eq. (3).

Open crack: The crack in a rotor system sometimes [10] has also been treated as an open crack, in case the vibrations are dominating to always keep the crack in the open condition. This results in a system are similar to an asymmetric shaft system.

2.2. Slant crack

The modelling of slant crack as explained in Ref. [7] is discussed here briefly. Consider a shaft element as shown in Fig. 3a. Applying torsional moment, M_z to a shaft causes primary stresses on its surface to lie orthogonal to each other at an angle of 45° towards the axis of the shaft. When a torsional vibratory moment is applied to the shaft under condition of smaller amplitude over a longer period, a slant crack can grow along the primary stress line as shown in Fig. 3b. The positive torsional moment puts the tensional stresses on the surfaces of the crack in such a way as to open it while the negative torsional moment applies compressional stress to close the crack.

Proceeding in a similar way as in reference Ref. [10] for a transverse crack, but considering the inclination of the crack while integrating, the compliance matrix for a slant-cracked section can be developed (see Ref. [7] for details). Using the principle of virtual work, the stiffness matrix of the cracked element can be obtained in a similar way as that of the transverse-cracked element.

The slant crack is generated because of torsional vibration, and opens and closes (i.e., "breaths") with torsional vibrations of the shaft. The moment of inertia of the section containing the crack will be higher when a negative moment is applied. As the bending stiffness of the shaft is proportional to the moment of inertia of the section of the shaft, we expect the bending stiffness of the shaft with the slant crack to change synchronously with the torsional vibration. The variation may be expressed by a truncated cosine series [7]:

$$[K] = [K(\omega_T t)] = [K_0] + [K_1]\cos(\omega_T t) + [K_2]\cos(2\omega_T t) + [K_3]\cos(3\omega_T t), \tag{4}$$

where $[K_\eta]$, $\eta = 0, 1, 2, 3$ are the fitting coefficient matrices determined from the known behaviour of the stiffness matrices at certain angular locations.

3. The equation of motion

The rotor system as shown in Fig. 1 is discretized in finite elements [12,13]. The equation of motion of the complete rotor system in a fixed coordinate system can be written as

$$[M]\{\ddot{q}\} + [D]\{\dot{q}\} + [K]\{q\} = \{Q\}. \tag{5}$$

The rotary and translational mass matrices of the shaft and the rigid disc mass, and the diametral moment of inertia are included in the mass matrix $[M]$. The matrix $[D]$ includes the gyroscopic

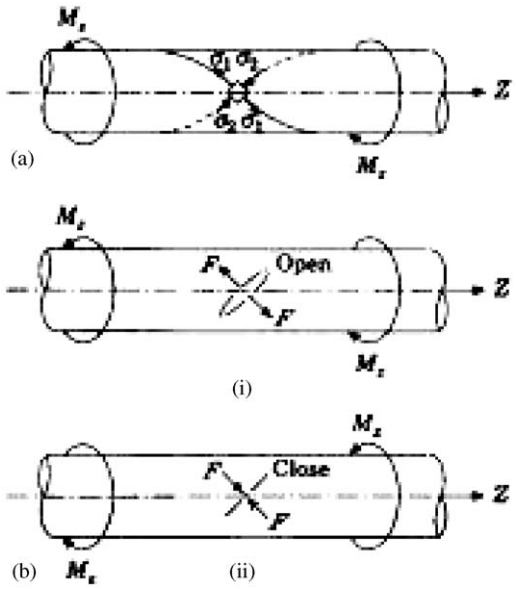

Fig. 3. (a) The primary stress directions of a shaft under torsional loading. (b) The breathing behavior of a slant crack: (i) $M_z>0$; (ii) $M_z<0$ [5,7].

moments and the bearing damping. The stiffness matrix considers the stiffness of the shaft elements including cracked shaft element and the bearing stiffness. For the analysis of cracked rotor system, the cracked element either with slant crack or with transverse crack will replace the element, which is initially uncracked. The excitation matrix $\{Q\}$ in Eq. (5) consists of the weight of the disc and the unbalance forces due to the disc having mass m, and eccentricity e. In the case of a slant crack a harmonically varying torsional moment with an amplitude M and torsional frequency ω_T also have been considered at the corresponding nodal degrees of freedom. The unbalance force components in x and y directions (F_x and F_y) for an angular position θ and a harmonically varying torsional moment (M_z) are given as

$$F_x = me\{\ddot{\theta}\ \sin\ \theta + \dot{\theta}^2\ \cos\ \theta\}, \tag{6}$$

$$F_y = me\{-\ddot{\theta}\ \cos\ \theta + \dot{\theta}^2\ \sin\ \theta\}, \tag{7}$$

$$M_z = M\ \sin\ (\omega_T t). \tag{8}$$

4. Dynamic analysis of cracked rotors

4.1. Eigenfrequencies

The crack is assumed to effect only stiffness. The stiffness matrix of a cracked element, $[K_c]$ will replace the stiffness matrix of the same element prior to cracking to result in the global stiffness

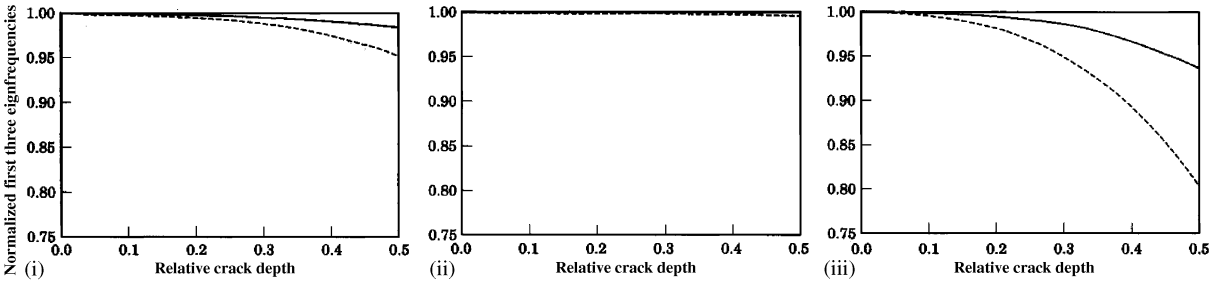

Fig. 4. Comparison of two types of cracks for eigenfrequencies, variation: — , slant crack ;----, transverse crack.

matrix $[\overline{K}]$ in Eq. (5). Thus, the eigenfrequencies and mode shapes are obtained by solving the eigenvalue problem $[K]-\omega^2\,[M]=0$, and $[\overline{K}]-\omega^2[M]=0$, for the uncracked and cracked rotor systems, respectively.

A rotor supported on two flexible bearings with a crack (slant/transverse) near to a central disc is considered (see Ref. [7] for details of data). The comparison of the two types of cracks for variation of eigenfrequencies with crack depth is shown in Fig. 4. The eigenfrequencies of cracked rotor are normalized with that of the uncracked rotor system while the crack depth is normalized with the shaft diameter ($\bar{\alpha}=(\alpha/D)$, where α is the crack depth in shaft diameter D or minor axis D). It can be observed from Fig. 4, that the eigenfrequencies reduce due to crack in both cases as the effective stiffness of the rotor system reduces. And also the decrease in eigenfrequencies depends on how close the crack is to the node of the corresponding mode shape (see Refs. [7,14] for more details). However, from Fig. 4 it can be noticed that the reduction in eigenfrequencies is smaller in the case of the slant cracked rotor.

4.2. Steady-state response

A lot of literature is available [1–4] on the steady-state response and behavior of a cracked rotor with transverse crack. It is very well understood that the FFT of such a response shows the characteristic features of $1X$, $2X$, $3X$ components of frequency equal to the rotor speed. However, the vibration behavior of the rotor with a slant crack is less understood. The points as discussed in Ref. [7] are mentioned here to compare these two types of cracks.

The steady-state response of the rotor system with a slant crack on its shaft induced by unbalance and a harmonically varying torsional moment contains frequencies represented by $\omega_n=m\Omega\pm n\omega_T/2$; $m=1,2,\ldots$ and $n=0,1,2\ldots$, where Ω is the operating speed of the rotor and ω_T is the frequency of torsional vibration of the rotor system. But the numerical results in Refs. [5,7] show that the above equation is satisfied only for even terms of 'n'. These frequencies are represented by $\omega_n=\Omega\pm n\omega_T$ for steady state.

4.3. Transient response

When the speed of rotation is changing, the angular rotation at any instant of time t can be taken as $\theta(t)=\Omega_0 t+1/2(at^2)$, where a is the angular acceleration of the rotor, Ω_0 is the initial angular velocity and t is the time. Time response can be obtained by using the Houbolt time marching.

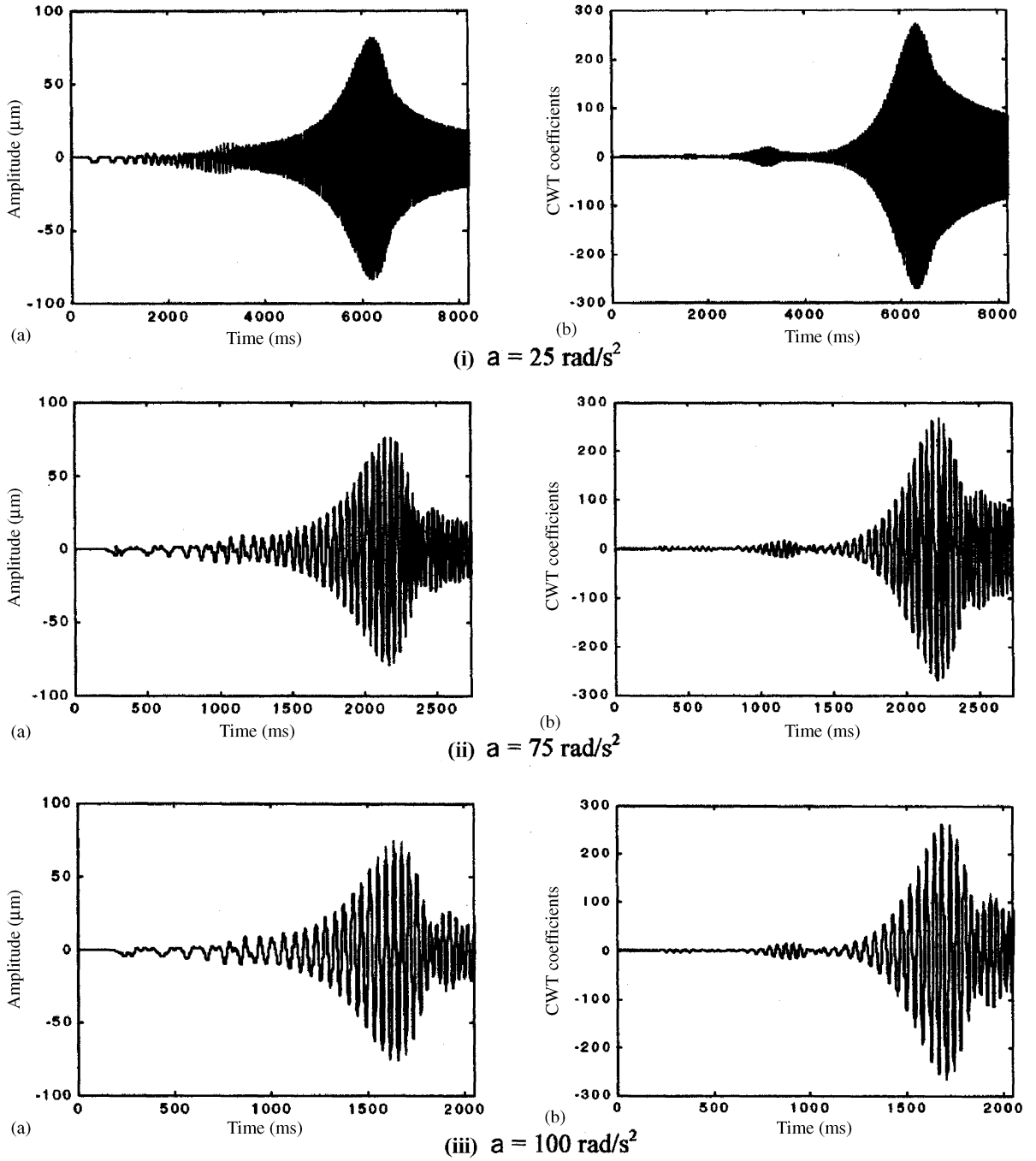

Fig. 5. Comparison of CWT at a scale of 35 with time response for different accelerations; $\bar{\alpha} = 0.3$; $X/L = 0.47$. (a) Time, (b) CWT.

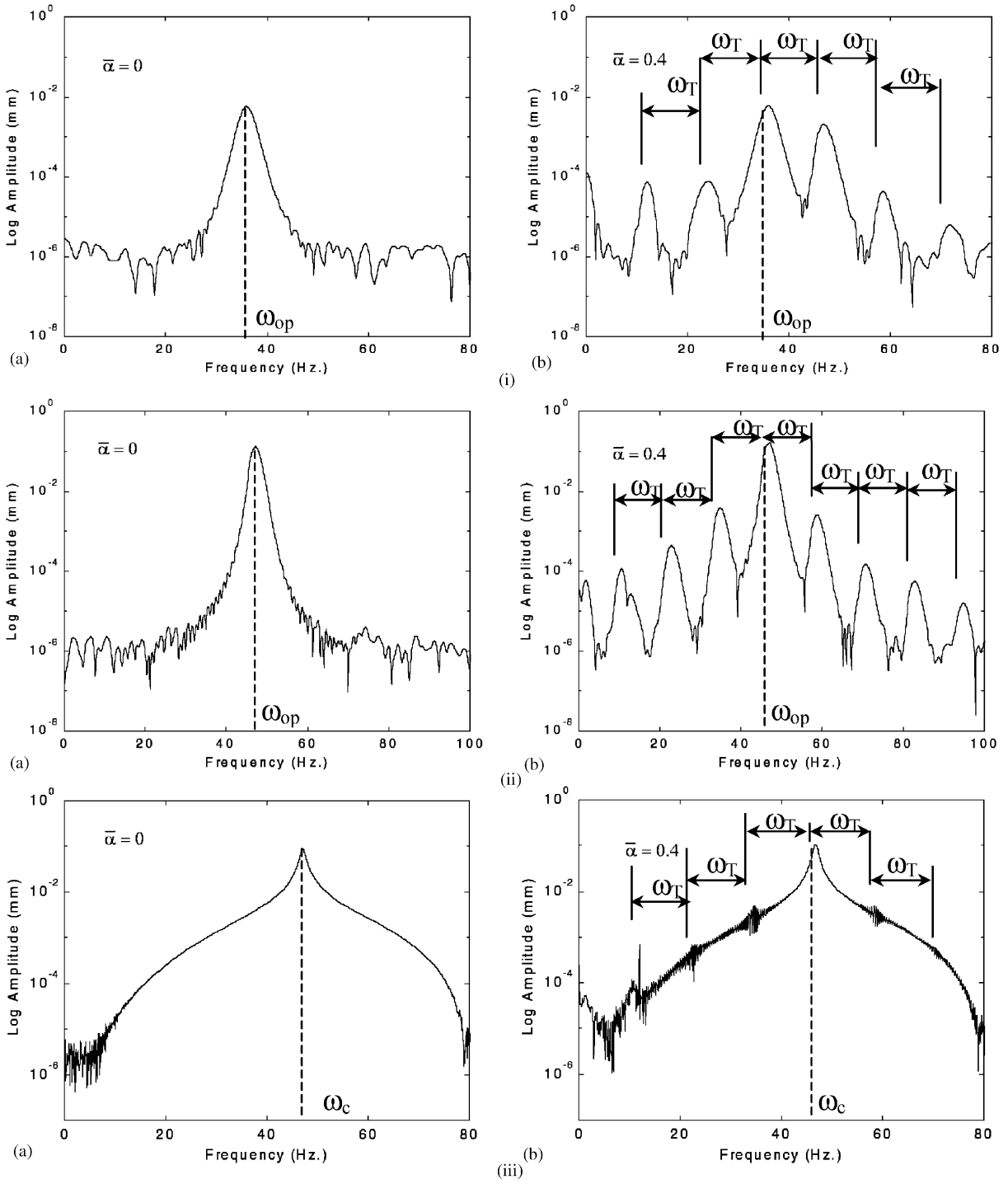

Fig. 6. Frequency response of the rotor (near disc) for windowed time responses at different locations in time signal; $a = 30\,\mathrm{rad/s^2}$; $\omega_T = 12\,\mathrm{Hz}$ [9]. (i) 7–8 s, (ii) 9.5–10.5 s, (iii) for entire time response. (a) $\bar{\alpha} = 0$, (b) $\bar{\alpha} = 0.4$.

Many works in Refs. [1–4] used speed- response, time domain signals and/or the traditional signal processing technique such as FFT for the analyses to detect cracks. The vibration signals during machine start-up or run-down are nonstationary (frequency changes with time) in nature. Wavelets provide time-scale information of a signal, enabling the extraction of features that vary in time. In a recent paper [15] the authors showed the effectiveness of wavelet transforms for crack detection and monitoring in rotors. The continuous wavelet transform (CWT) has been applied to extract the features of transverse cracks from the time domain signals of the rotor-bearing system. The time responses obtained at the disc location did not show clear symptoms of crack. However, the characteristic sub-critical response peak can be clearly observed in the CWT of the cracked rotor system. A typical result as shown in Fig. 5, indicates the effectiveness and importance of the CWT, particularly at higher acceleration of the rotor.

In the case of a transverse crack, the frequency of breathing is varying with rotating speed, while the rotor passes the critical speed. But in the case of slant crack, the breathing behavior of the crack is due to torsional vibrations where it has been assumed that the torsional frequency is constant irrespective of the rotating speed. Hence, torsional frequency components are not extracted using CWT for detection of the slant crack in a rotor system. However, the FFT of the time response similar to the steady state has been used for slant crack detection (see more details in Ref. [9]). A rotor-bearing system with slant crack subjected to a harmonically varying torsional moment with amplitude of 1.5 N-m and passing through its critical speed with angular acceleration of 30 rad/s^2 has been considered. The time response has been multiplied by window function to get better frequency components in frequency spectrum (obtained by FFT).

Fig. 6 shows the frequency spectra taken for 1 s windowed time response before and during passing of the critical speed of the rotor (see Fig. 6(i–ii)). The frequency spectra have also been taken for entire windowed time response of the rotor as shown in Fig. 6(iii). Since, the angular acceleration is 30 rad/s^2, there are synchronous frequencies at 35.8 and 47.75 Hz (referred as instant operating speed, ω_{op}) in the frequency responses of the three windowed time responses. The synchronous frequency in Hz is given by angular acceleration of the rotor times the average of 1 s windowed time/2π.

As in the steady-state case [7], when the crack is present in the shaft, it can be observed that the sub- and super-harmonic frequency components at an interval of torsional frequency are centered on the above frequency peaks as shown in Fig. 6(i–iii). So vibrations of a rotor with the slant crack can be compared with the steady-state case until the rotor is not passing the critical speed. As soon as the cracked rotor passes the critical speed, the sub-harmonics in the frequency spectrum of entire time response centers on the critical speed ($\omega_c = 47$ Hz) because of the high vibrations in the critical speed region (see Fig. 6(ii–b)). Thus, it is found that the unbalance response of a slant cracked rotor passing through its critical speed contains frequencies represented by $\omega = \omega_c \pm n\omega_T$ where ω_c is the first critical speed of the rotor system.

5. Detection and monitoring of cracks

The transverse crack can be identified through the characteristics of $2\times$ and $3\times$ components of running speed frequency. In the case of transient rotors, the cracks can be detected and monitored using the wavelets (CWT) as explained in Section 4.3. The slant crack in a different

way, can be identified, by observing the sub-and super-harmonic components, centering the operating or critical speed at an interval of torsional frequency (see Sections 4.2 and 4.3).

Apart from the wavelet techniques, crack detection through mechanical impedance [16] has also been used for transverse cracks. This method has also been validated through experiments [17]. The mechanical impedance is very effective in detection of a crack, as it has been shown to be very sensitive to a crack. However, this method has not been tested for the slant crack rotor before. The results are present here.

The rotor shaft is discretized into finite beam elements as shown in Fig. 1 (even though the figure shows the transverse crack, the same is applicable for the slant crack). The rotor data are provided in Table 1. In the present work, an external impulse force of constant magnitude of 15 N for a short duration of time (0.01 s) has been applied on the rotor-bearing system in addition to unbalance and a harmonically varying torsional moment. Mechanical impedance $Z(X_f)$ of the rotor-bearing system at any force location 'X_f' from the left bearing location (see Fig. 1) is defined as the ratio of force $F(X_f)$ to the velocity response $V(X_f)$ at the same location. Mathematically,

$$Z(X_f) = F(X_f)/V(X_f). \tag{9}$$

The normalized mechanical impedance is defined as the mechanical impedance of the rotor system with a crack (Z_c) to that of without a crack (Z_0). The mechanical impedance $Z(X_f)$ is obviously a function of frequency.

Table 1
Rotor system data for impedance analysis for the slant crack

Length of the rotor, L	50 cm
Shaft	
Diameter, D	2 cm
Density and modulus of elasticity	7800 kg /m^3, 2.08E11 N/m^2
Disc	
Location	Mid-span
Mass, m	5.5 kg
Polar moment of inertia, I_p	0.01546 kg m^2
Diametral moment of inertia, I_D	0.00773 kg m^2
Unbalance eccentricity, e	0.1 mm
Crack	
Location, X/L	0–0.5
Depth, $\bar{\alpha}(\alpha/D)$	0.1–0.4
Bearing (isotropic)	
Stiffness	10^5 N/m
Damping	100 Ns/m
Force (F)	
Magnitude	15 N
Duration	0.01 s
Location, X_f/L	0.04–0.5
Operating speed of rotor	9.55 Hz
Torsional frequency	3.94 Hz
First eigenfrequency	24.27 (Hz)

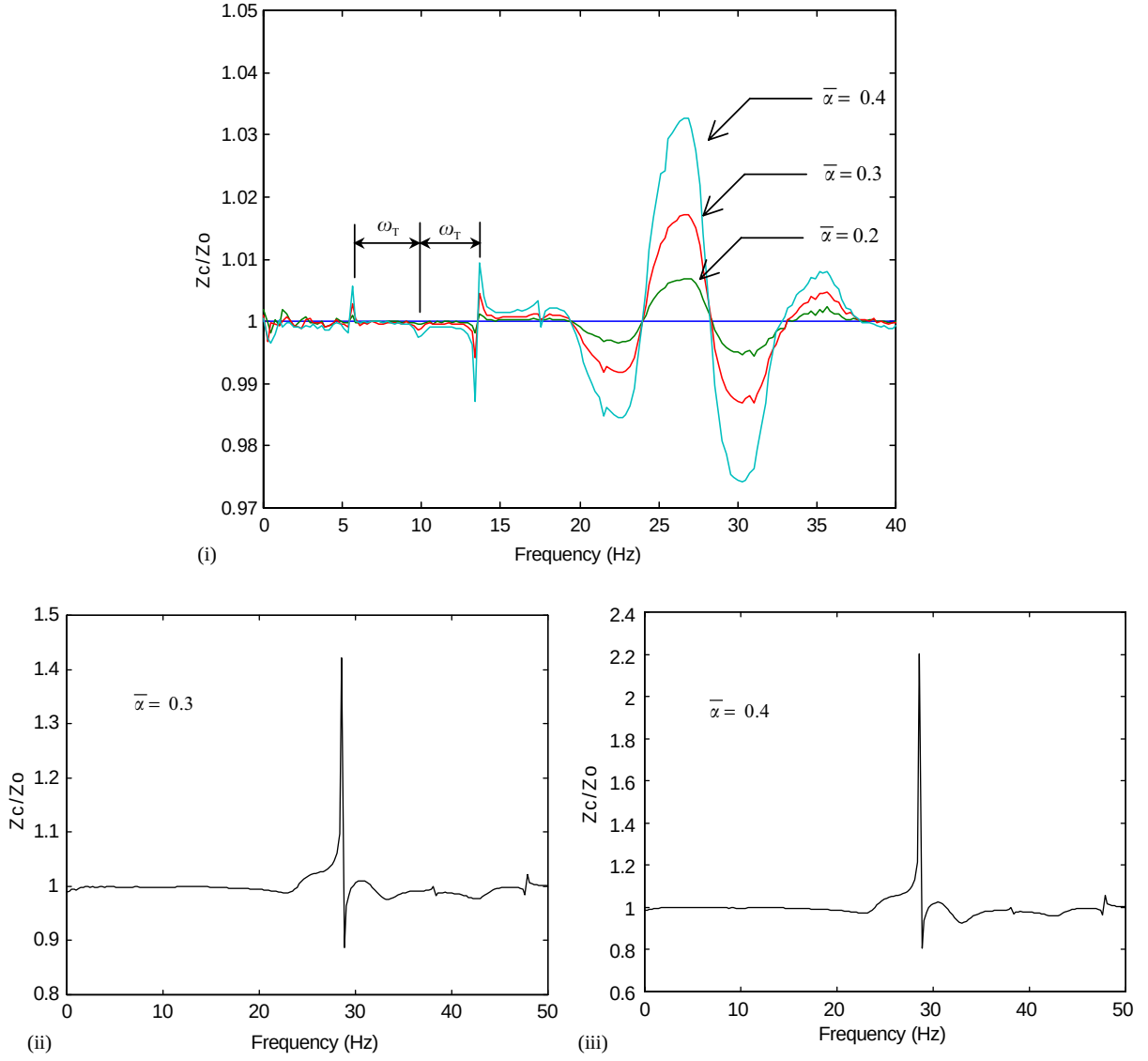

Fig. 7. (i) Variation of impedance with frequency for different slant crack depths; $X_f/L = 0.04$; $X/L = 0.43$; $\omega_T = 3.97$ Hz. (ii) Variation of impedance with frequency for different transverse crack depths; $X_f/L = 0.04$; $X/L = 0.43$.

A parametric study has been conducted for the rotor system by considering slant crack, which is assumed to breathe with a torsional frequency of 3.94 Hz.The variations of impedances with frequency for different crack depths by keeping crack and force locations unchanged are shown in Fig. 7(i). Even though the change of impedance has been observed over the range of frequencies, the substantial changes of mechanical impedance are found at natural frequency, running frequency and also at some significant frequencies (see Table 1). The significant frequency components are at an interval frequency corresponding to torsional frequency (3.94 Hz) and

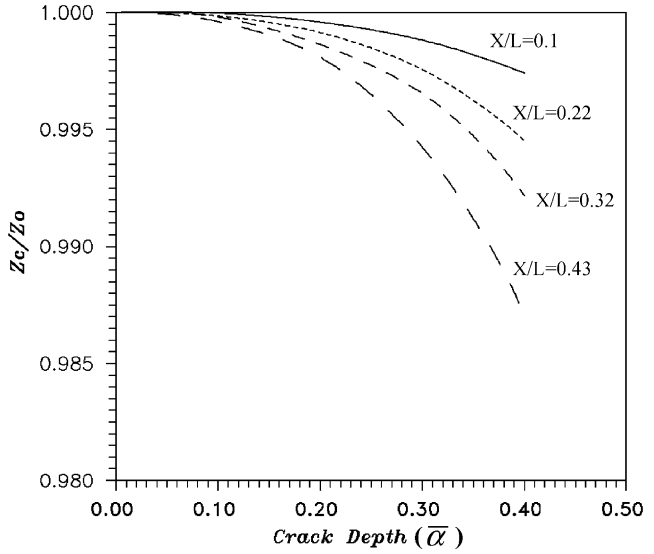

Fig. 8. Variation of impedance with crack depth for different slant crack locations at frequency = 13.43 Hz; $X_f/L = 0.04$; $\omega_T = 3.97$ Hz.

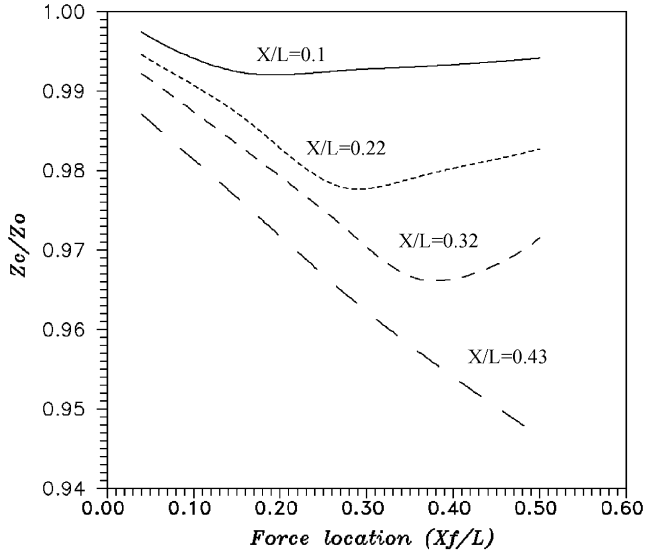

Fig. 9. Variation of impedance with force location for different slant crack locations at frequency = 13.43 Hz; $\bar{\alpha} = 0.4$; $\omega_T = 3.97$ Hz.

found to be centered on operating speed (9.55 Hz) of the rotor system. This is happening due to the breathing action of the slant crack with torsional frequency. From Fig. 7(i), it can be seen that there is a slight shifting of peaks at natural frequencies (near 24.27 Hz) towards lower values, as the crack depth increases. This is due to the reduction in the stiffness because of increase in crack

depth. However, it is observed from the same figure, that the impedance change is much more and thus is more sensitive to crack.

The impedance changes in this case have been compared with those of the transverse crack case [16] as shown in Figs. 7(i–ii). It can be noticed from Figs. 7(i and ii) that the normalized mechanical impedance change is highly sensitive to depth in the case of transverse crack as compared to impedance change of the rotor system due to the slant crack (Fig. (i)).

Fig. 8 shows the variation of mechanical impedance at the frequency of 13.43 Hz with crack depth, for different crack locations. Mechanical impedance decreases as the crack depth increases significantly. The effects of force location on impedance are shown in Figs. 9 and 10. At all the locations, the breathing action of the crack can be clearly identified by the sudden change of mechanical impedance at the significant frequencies, natural frequency and running frequency (see Fig. 10(i)). The mechanical impedance changes substantially over the range of frequencies as the force location moves towards the disc and the crack is near the disc. The trend is also same for

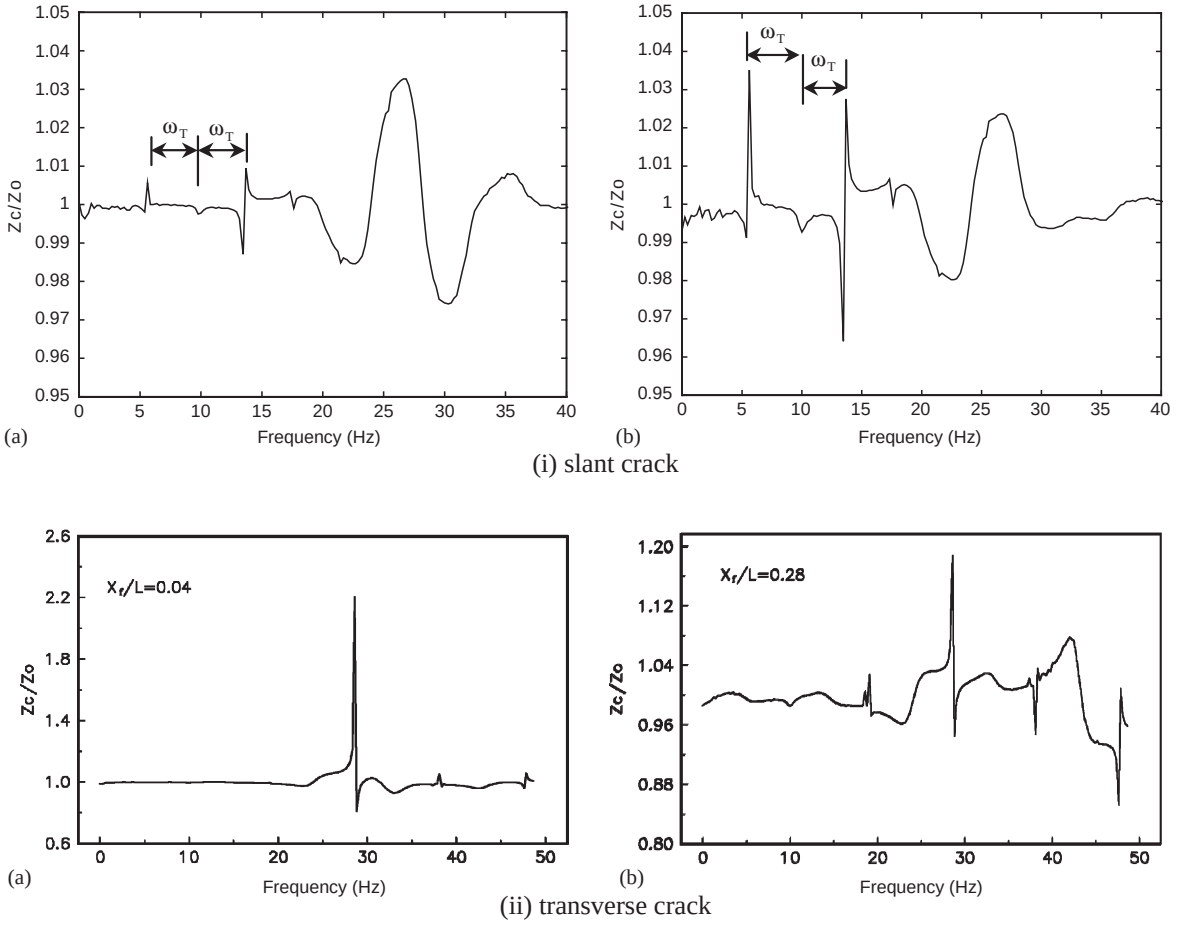

Fig. 10. Variation of impedance with frequency for different force locations and cracks: $\bar{\alpha} = 0.4$; $X/L = 0.43$; $\omega_T = 3.97$ Hz. (a) $X_f = 0.04$; (b) $X_f = 0.28$.

the transverse crack case [16], i.e. the impedance decreases until the force application point crosses the crack and then increases gradually as the force moves toward the disc (see Fig. 9). However, the normalized mechanical impedance change is highly sensitive to depth in the case of transverse crack, which is clear from the Fig. 10 in addition to Fig. 7. As observed for structures, the mechanical impedance of the rotor system could be used as additional information for crack detection since it depends on the position at which it is measured. Although, the mechanical impedance change is more sensitive in the case of transverse crack (see Figs. 7 and 10), the change is significant in the case of slant crack also as compared to natural frequency change. Hence, this technique can also be used for slant crack detection.

6. Summary

The detection and monitoring of slant crack in the rotor system using mechanical impedance has been presented in this paper. The effect of a slant crack parameters on normalized impedance (Z_c/Z_0) is the same as transverse cracks, but a transverse crack is highly sensitive to mechanical impedance compared to a slant crack. The changes in rotor impedance due to cracks are

Table 2
Comparison of transverse crack with slant crack

Sl. no	Phenomenon	Transverse crack	Slant crack
1	Breathing (opening and closing of crack)	Crack breaths with a frequency equal to rotation of shaft (ω)	Crack breaths with a frequency equal to torsional excitation frequency (ω_T)
2	Effect on eigenfrequencies	Eigenfrequencies reduce due to crack significantly	Reduction in eigenfrequencies due to crack is relatively less
3	Steady-state response	FFT shows the characteristic features of $1X$, $2X$, $3X$ components of frequency equal to the rotor speed	FFT shows the sub-and super-harmonic frequency components at an interval frequency corresponding to torsional frequency centering on the rotor running frequency
4	Transient analysis	The wavelets can be used effectively for crack detection	Vibrations of cracked rotor can be compared with steady-state case (point 3), until the rotor does not pass the critical speed
		Sub-harmonic resonant peaks are clearly seen in the CWT of the transient response	As soon as the cracked rotor passes the critical speed, the side bands corresponding to torsional frequency center on the critical speed
5	Response to impulse	The normalized mechanical impedance is highly sensitive to crack depth	The normalized mechanical impedance is relatively less sensitive to crack

significant, as compared to that of natural frequencies of the rotor-bearing system. The results suggest that the measurements of mechanical impedance can also be used for slant crack detection and monitoring.

The paper synthesizes several works of the authors on cracked rotors. The vibration behavior of rotors with types, viz., the transverse crack and slant crack has been discussed through the modeling; the dynamic analysis; and detection and monitoring techniques. The summary of the comparison of the two types of shaft cracks is given in Table 2. The study shows that detection of crack in the rotors can be done effectively by applying suitable methods depending on the operational behavior.

References

[1] A.D. Dimarogonas, S.A. Paipetis, *Analytical Methods in Rotor Dynamics*, Applied Science Publishers, London, 1983 pp. 144–193.
[2] J. Wauer, Dynamics of cracked rotors: literature survey, *Applied Mechanics Reviews* 43 (1990) 13–17.
[3] R. Gaush, A survey of the dynamic behavior of simple rotating shaft with a transverse crack, *Journal of Sound and Vibration* 160 (1993) 313–332.
[4] A.D. Dimarogonas, Vibration of cracked structures: a state of the art review, *Engineering Fracture Mechanics* 55 (1996) 831–857.
[5] M. Ichimonji, S. Watanabe, The dynamics of a rotor system with a shaft having a slant crack (a qualitative analysis using a simple rotor model), *JSME International Journal, Series III* 31 (4) (1998) 712–718.
[6] M. Ichimonji, Y. Kazao, S. Watanabe, S. Nonaka, The dynamics of a rotor system with slant crack under torsional vibration, in: *Nonlinear and Stochastic Dynamics, Proceedings of the ASME International Mechanical Engineering Congress and Exposition*, Chicago, IL, 1994, pp. 81–90.
[7] A.S. Sekhar, P. Balaji Prasad, Dynamics of a rotor system considering a slant crack in the shaft, *Journal of Sound and Vibration* 208 (3) (1997) 457–474.
[8] A.S. Sekhar, Condition monitoring of a rotor system having a slant crack in the shaft, *Noise & Vibration Worldwide* 30 (3) (1999) 23–31,1999.
[9] S. Prabhakar, A.S. Sekhar, A.R. Mohanty, Transient analysis of a slant-cracked rotor passing through its flexural the critical speed, *Mechanism and Machine Theory* 37 (9) (2002) 1007–1020.
[10] C.A. Papadopoulos, A.D. Dimarogonas, Coupled longitudinal and bending vibrations with an open crack, *Journal Sound and Vibration* 117 (1987) 81–93.
[11] A.S. Sekhar, B.S. Prabhu, Transient analysis of a cracked rotor passing through the critical speed, *Journal of Sound and Vibration* 173 (1994) 415–421.
[12] H.D. Nelson, J.M. McVaugh, The dynamics of rotor-bearing systems using finite elements, *Journal of Engineering for Industry* 98 (2) (1976) 593–600.
[13] H.N. Ozguven, Z.L. Ozkan, Whirl speeds and unbalance response of multi bearing rotor using finite elements, *Journal of Vibration, Acoustics Stress and Reliability in Design* 106 (1984) 72–79.
[14] A.S. Sekhar, B.S. Prabhu, Crack detection and vibration characteristics of cracked shafts', *Journal of Sound and Vibration* 157 (2) (1992) 375–381.
[15] S. Prabhakar, A.S. Sekhar, A.R. Mohanty, detection and monitoring of cracks in a rotor-bearing system using wavelet transforms, *Mechanical Systems and Signal Processing* 15 (2) (2001) 447–450.
[16] S. Prabhakar, A.S. Sekhar, A.R. Mohanty, Detection and monitoring of cracks using mechanical impedance of rotor-bearing system, *Journal of the Acoustical Society of America* 110 (5) (2001) 2351–2359.
[17] S. Prabhakar, A.R. Mohanty, A.S. Sekhar, Crack detection by measurement of mechanical impedance of a rotor-bearing system, *Journal of the Acoustical Society of America* 112 (6) (2002) 2825–2830.